The influence of microstructure characteristics on electrical properties in ITO thin film

Chenggang Yang [1], *Jingyuan* Yang [1,*], *Dongao* Han [1], *Chan* Li[1] ,*Yuting* Xu [1], and *Yang* Qiu[2]

[1]Nuclear and Radiation Safety Centre MEE, Beijing 102400, China
[2]NICE Solar Energy Corporation Ltd., Beijing 102211, China

Abstract: ITO thin films were deposited on sapphire substrates under different deposition parameters via ion-assistant electron beam evaporation method. Microstructure characteristics such as crystalline structure and surface morphology of as-deposited ITO thin films were studied by using X-ray diffraction spectroscopy, transmission electron microscopy and field emission scanning electron microscopy, as well as the index of sheet resistance, carrier concentration, carrier mobility and transmission in visible spectrum were tested by means of Hall effect tester and UV-VIS-NIR spectrophotometer, respectively. The influence and impact mechanism of microstructure characteristic on electrical properties of as-deposited ITO thin films were investigated and analyzed in detail.

1 Preface

Sn doped In_2O_3 (ITO) [1] is a kind of semiconductor oxide thin film [2,3]. Due to the excellent combination of wide band gap (> 3.5 eV [4]), low resistivity, high transmittance in visible spectrum (> 95% at 550 nm), high IR reflectance (> 80%) and other unique physical properties[5], ITO thin films were widely used in varieties of industries such as flat panel displays, LEDs, solar panels, thermal mirrors, electrochromic devices [6,7], etc.

In all of the applications, ITO thin films are required to present excellent electric and optical properties. For this reason, researchers have spent great efforts on investigating ITO's electrical and optical properties during last several decades. However, due to the coating mechanisms of different deposition methods and the complex effects of various process parameters involved in, the electrical and optical properties of ITO thin films often conducted diversely or even inversely to the deposition parameters according to the past research works. As a result, there is still controversy in the understanding to the mechanisms of electrical and optical properties of ITO thin films. Therefore, further studies on the electrical and optical properties of ITO thin films still show great significance. The theoretical calculation shows that the carrier mobility of In_2O_3 single crystal can be as high as 160 $cm^2V^{-1}s^{-1}$[8], therefore, the resistivity of ITO thin films can be as low as 4.4×10^{-6} $\Omega \cdot cm$ theoretically. Practically, Suzuki et al. [9] obtained high-quality ITO thin film via PLD method at 300℃, the transmittance in visible spectrum was over 90%, the resistivity was as low as 7.2×10^{-5} $\Omega \cdot cm$, and the carrier mobility was as high as 2.5×1021 cm^{-3}; Ohta et al[10]

studied ITO thin film with ultra-flatness and intense (400) texture which was epitaxial grown on single crystal YSZ (Yttria-Stabilized Zirconia) substrate at 600℃ via PLD, and its resistivity was as low as 7.7×10^{-5} $\Omega \cdot cm$, the carrier mobility was as high as 1.9×1021 cm^{-3}, and the Hall mobility was 44 $cm^2V^{-1}s^{-1}$, which was the most remarkable electrical property obtained by conventional methods reported in the literature. It can be seen that there is still a large gap between the current electrical properties of ITO thin films and theoretical calculation, which indicates that more profound researches are still indispensable. Therefore, studies on precise control of the electrical and optical properties of ITO thin films are particularly significant.

In this paper, ITO thin films were deposited on sapphire substrates under different deposition parameters via ion-assistant electron beam evaporation method. Microstructure characteristics such as crystalline structure and surface morphology of as-deposited ITO thin films were studied by using X-ray diffraction spectroscopy, transmission electron microscopy and field emission scanning electron microscopy, as well as the index of sheet resistance, carrier concentration, carrier mobility and transmission in visible spectrum were tested by means of Hall effect tester and UV-VIS-NIR spectrophotometer, respectively. The influence and impact mechanism of microstructure characteristic on electrical properties of as-deposited ITO thin films were investigated and analyzed in detail.

2 Experiment

---

* Corresponding author: yjyle@163.com

2.1 Sample preparation

ITO thin films were deposited by ion-assisted electron beam evaporation (EB). During the deposition process, O_2 with high purity was introduced into the cathode of Hall ion source and was ionized by high-speed electron bombardment, the O- beam formed was utilized to ion cleaning and ion assistance during the deposition. The O_2 flow was regulated by the mass flow control meter (MFC). Sapphire (Φ=15 mm, d=2 mm) was used as substrate, and ultrasonically cleaned with acetone, alcohol and deionized water in sequence, and then fixed on the fixture after drying. Before deposition, the chamber was evacuated to a background vacuum of 9.0 ×10-5Pa, the substrates were heated to 300℃ and baked for 30 minutes. ITO particles with high purity were used as the evaporation material (In_2O_3:SnO_2=9:1 %, D=1~4 mm, Umicore). 270° E-type electron gun was used as the thermal source, the deposition rate was adjusted by regulating the current of electron beam. The film thickness and deposition rate were monitored by the quartz crystal microbalance (QCM) in real-time. ITO thin films were deposited under different deposition parameters. First, the oxygen flow rate was fixed at 45sccm, and the ITO thin films were deposited at deposition rates of 1Å/s, 2Å/s, 3Å/s, and 4Å/s. Samples were marked as: R1~ R4; Secondly, the deposition rate was fixed at 2Å/s, and the depositions were conducted under oxygen flow rates of 30, 40, 50 and 60sccm, respectively. Samples were marked as: O_{30}~O_{60}. The thickness of the films was set to 250 nm, and no post annealing treatment was implemented afterwards.

2.2 Characterization

The microstructure characteristics of ITO thin films were characterized by X-ray diffractometer (XRD, Bruker D8 advance). The test conditions were as follows: Cu target Kα radiation, λ=0.15406 nm, θ-2θ scanning method, scanning range was 10º~80º. The transmission electron microscope bright-field image and selected area electron diffraction (SAED) spectrum of thecross-section were tested by FEI Tecnai T20 transmission electron microscope. The morphology was taken by Hitachi S-4800 field emission scanning electron microscope (FE-SEM). The sheet resistance, resistivity, carrier concentration and carrier mobility at room temperature were tested by means of Van der Pauw method via HL5500PC Hall tester (Nanometrics Inc.). Voltage: 20 mV; DC: 1 mA; magnetic field strength: 0.53 T. The transmittance of ITO thin film in the visible spectrum was measured by Shimadzu UV-3600 UV-VIS-NIR spectrophotometer with a resolution of 1 nm.

3 Results and discussions

3.1 Structural characteristics

XRD pattern of the ITO thin films obtained is shown in Figure 1. The comparison with the standard PDF card JCPDS 06-0416 shows that ITO thin film as-deposited are polycrystalline, with body-centered cubic structure (bixbyite, spatial point group: Ia-3 No.206) and (222) textured. The film grain size (see Table 1) D is estimated by Scherrer formula[11].

$$D = \frac{0.9\lambda}{\beta \cdot \cos\theta} \quad (1)$$

where, λ is the wavelength of the X-ray used for testing, β is the FWHM (full width at half maximum) of the diffraction peak corresponding to a certain 2θ angle. The calculation result shows that the average grain size of the ITO thin films increases with the increasing of deposition rate, while the variation of oxygen flow rate shows no obvious influence on the grain size.
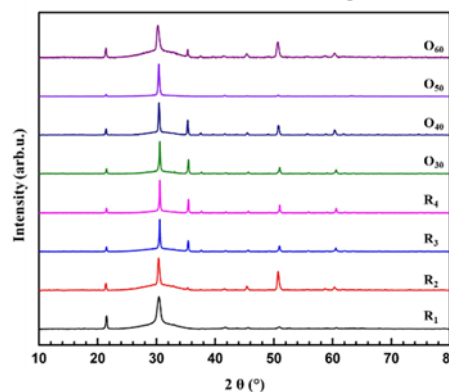

Fig.1 XRD pattern for ITO thin films deposited at different parameters.

Table 1. Physical properties of as-deposited ITO thin films

	R₁	R₂	R₃	R₄	O₃₀	O₄₀	O₅₀	O₆₀
Grain size (nm)	65.2	70.4	85.8	110.7	74.0	82.7	72.9	124.1
Sheet resistance (Ω/□)	28.5	11.9	18.3	21.7	21.7	27.1	10.3	10.1
Resistivity (10^{-4} Ω·cm)	7.14	2.99	4.57	5.42	5.43	6.77	2.58	2.53
Electron mean free path (nm)	11.8	3.9	3.8	4.1	5.2	7.5	3.3	2.9

It can also be observed from Figure 1 that the diffraction peak intensity of the (400) crystal plane of the ITO thin films gradually increases with the increasing of deposition rate, and decreases with the increasing of oxygen flow rate within the range of 30-50 sccm, but rises slightly at oxygen flow rate of 60 sccm. The enhancement of the texture on (400) plane is usually caused by the increasing in the concentration of oxygen vacancies. In the experiment, with the increasing of the growth rate or the decreasing of the oxygen flow rate,

the relative oxygen content along the growth surface of the film gradually decreased, resulting in an increase in the growth trend along (400) crystal plane in the film; On the other hand, when the oxygen flow rate reached 60 sccm, The oxygen flow per unit time exceeded the upper limit for the ionization capability of the Hall source. The surplus oxygen atoms led pressure in the vacuum chamber to rise, which reduced the mean free path of oxygen ions, prevent the oxygen ions from reacting with the growing film completely, and increased the oxygen vacancy concentration, led the film to grow along the (400) plane to a certain extent.

In addition, the XRD peaks of sample R_1 and R_2 both show a certain degree of broadening. D. Mergel et al. [11] believes that this is caused by the segregation of neutral SnO_2 at the grain boundaries of the film in the oxygen-rich environment. In the experiment, R_1 was selected as the sample of TEM test. The SAED spectrum of the cross-section is shown in Figure 2(a). The inset is the TEM brightfield image of the selected area. We can see that in addition to the (211), (222), (400), (440) and (622) crystal plane diffraction rings of cubic In_2O_3, dim diffraction spots can also be observed at the position indicated by the arrow, with d values of 3.31 Å, 3.34 Å, and 3.32 Å (Figure 2 (b), (c), (d)). Among the possible composite, only the (110) crystal plane (d=3.3470 Å, JCPDS 41-1445) of tetragonal SnO_2 has corresponding interplanar spacing value. This indicates that there are SnO_2 crystallites in the film, but due to the relatively low content, no obvious diffraction peaks can be observed in

the XRD pattern. The possible reason for its formation is that when the deposition rate is low, the growth surface of the film is in a relatively oxygen-rich environment, and a fraction of Sn ions are oxidized and segregate at the grain boundaries by the form of neutral SnO_2.
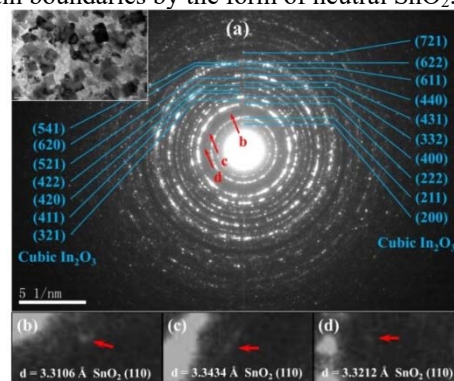

Fig.2 SAED image of ITO thin film. Inset at top left corner shows corresponding bright field image of ITO thin film, appended images (b), (c), (d) show the diffraction spots of SnO2 (110).

Figure 3 shows SEM morphology photos of ITO thin films prepared under different parameters. We can see that the grain size of the ITO thin film increases with the increasing of deposition rate, which is consistent with the calculation results in the above XRD analysis. With the increasing of the deposition rate, the surface of the film becomes rougher and structural defects increase.
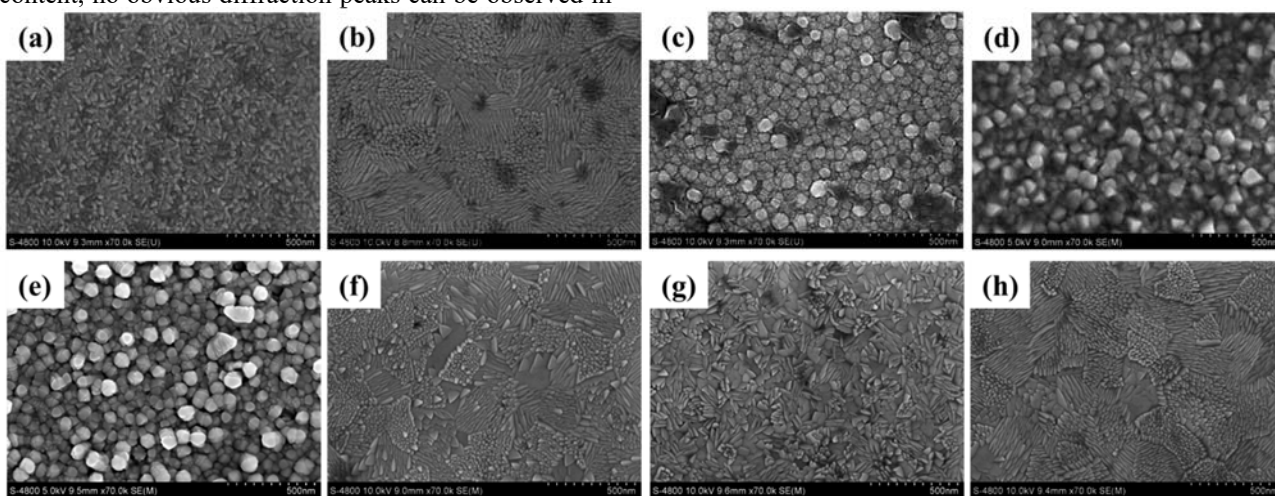

Fig.3 SEM images of ITO thin films deposited at different parameters.

3.2 Electrical Performance

The sheet resistance and resistivity of the ITO film tested by the Van der Pauw method are listed in Table 1. For semiconductor transparent conductive oxide film materials, the resistivity ρ and conductivity σ are in reverse proportion to each other:

$$\rho = \frac{1}{\sigma} = \frac{1}{Ne\mu} \qquad (2)$$

Where, N is the carrier concentration, e is the electron charge, μ is the carrier mobility. This formula shows that the electrical properties of the ITO thin film are determined by the carrier concentration and carrier mobility, the doping characteristics and carrier scattering mechanism that restrict the above two factors are mainly affected by the microstructure characteristics of the film. Figure 4 (a) and (b) are the carrier concentration and carrier mobility in ITO thin films prepared under different deposition rates and oxygen flow rates,

respectively. As can be seen from the figure, as the deposition rate increased, the carrier concentration of the ITO film gradually increased, Samples R_1~R_4 are 3.38×1020 cm^{-3}, 4.82×1020 cm^{-3}, 9.17×1020 cm^{-3} and 1.1×1021 cm^{-3} respectively. The carrier concentration

decreased initially and increased afterwards with the increasing of oxygen flow rate, O_{30}~O_{50} are 7.60×1020 cm^{-3}, 6.11×1020 cm^{-3}, 5.06×1020 cm^{-3} and O_{60} is 5.80×1020 cm^{-3} respectively.
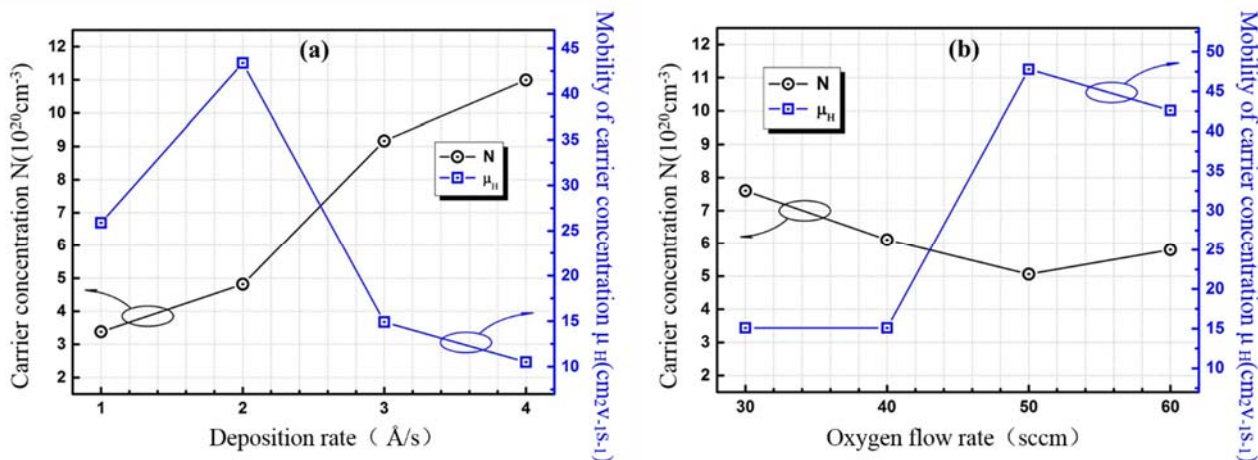

Fig.4 Electrical properties of as-deposited ITO thin films

In ITO thin film, the main sources of carriers are intrinsic oxygen vacancies and the substitutional doping of Sn^{4+} to In^{3+}. XRD test results show that the increase in the deposition rate enhances (400) texture in the film, which indicates that the oxygen vacancy concentration in the film increases with the increasing of deposition rate. The film grows in a relatively oxygen-rich environment at a low deposition rate, the evaporated particles are fully oxidized making the oxygen vacancy concentration small in the film, the relatively oxygen-deficient environment formed during the growth of the high deposition rate film increases the concentration of oxygen vacancies in the film; In addition, the broadening of the diffraction peaks in the XRD spectrum and the results of TEM selected area electron diffraction indicate that there is neutral SnO_2 segregation at the grain boundaries of the sample R_1 and R_2 films, which reduce thedoping concentration of Sn^{4+} to In^{3+} in the lattice. The high deposition rate shows little effect on the doping ratio of Sn^{4+}. Therefore, the carrier concentration of the ITO thin film in the experiment increases with the increasing of deposition rate. In the oxygen flow experiment, the intense (400) peak in the XRD spectrum shows that the carriers of samples O_{30} and O_{40} are mainly derived from high-concentration oxygen vacancies formed during the deposition process of low oxygen flow. And because the oxygen flow rate is small during the deposition process, the oxygen ion-assistant energy is relatively low, which is not conducive to the formation of substitutional doping of Sn^{4+} in the film lattice, The carrier concentrations of O_{30} and O_{40} are less than R_3 and R_4. And for sample O_{50}, the crystal plane diffraction peaks of strong (222) and very weak (400) appearing in the XRD spectrum indicate that the concentration of oxygen vacancies in the film is low, But the increase in oxygen flow increases the auxiliary energy of oxygen ions, making Sn^{4+} obtain higher energy during the deposition process to enter the crystal lattice

to form substitutional doping. Therefore, the carrier concentration in O_{50} is lower than O_{30}, O_{40} and slightly higher than R_2. The increase in the carrier concentration of the sample O_{60} is due to the increasing in the amount of oxygen during the deposition process, which increases the pressure in the vacuum chamber, reduces the mean free path of ion, resulting in the reduction of the assistant energy of oxygen ions, the film atoms are not fully oxidized, the oxygen vacancy concentration in the film slightly rises, and appears as a relative enhancement of the diffraction peak (400) in the XRD spectrum..

The carrier mobility of the ITO film increases first and then decreases with the increasing of deposition rate, from 25.9 cm^{2}V^{-1}s^{-1} for R_1 to 14.9 cm^{2}V^{-1}s^{-1} for R_2 and 10.5 cm^{2}V^{-1}s^{-1} for R_3 and R_4. On the other hand, the carrier mobility of the film changes with the amount of oxygen flow rate from 15.1 cm^{2}V^{-1}s^{-1} of O_{30} and O_{40} rise to 47.8 cm^{2}V^{-1}s^{-1} of O_{50} and then slightly down to 42.6 cm^{2}V^{-1}s^{-1} of O_{60}.

The significant decrease in carrier mobility of thin film samples in the experiment can be attributed to the ionized impurity scattering mechanism[12]. For samples with higher carrier concentration, R_3, R_4, O_{30} and O_{40}, high-concentration substitutional doping and the formation of oxygen vacancies cause a large number of ionized impurity centers in the film, and an additional short-range potential will form around it, which will disturb the electromagnetic field in vicinity, hinder carrier transport, and reduce carrier mobility. The ionized impurity scattering mechanism in the transparent conductive semiconductor film can be described by equation:

$$\mu_{HS} = \frac{4e}{h}\left(\frac{\pi}{3}\right)^{\frac{1}{3}} N^{-\frac{2}{3}} \qquad (3)$$

Where, h is Planck constant, N is the carrier concentration in the film, it can be seen from equation (3)

that the attenuation of ionized impurity scattering on carrier mobility increases with the increasing of carrier concentration. At the same time, higher doping concentration can also cause lattice distortion, destroy the periodic potential field of electron cloud, and form the static lattice defect scattering. On the contrary, the carrier concentration in sample R_1, R_2, O_{50} and O_{60} is relatively lower, and ionized impurity scattering and lattice defect scattering have relatively less effect on carrier mobility.

Since the ITO thin film is n-type semiconductor material which carriers are free electrons, and the mean free path of electrons in the film can be calculated using the heavily doped semiconductor electron cloud model[13]:

$$L = (3\pi^2)^{\frac{1}{3}} \cdot h \cdot e^{-2} \cdot \sigma \cdot N^{\frac{2}{3}} \quad (4)$$

Where, h is the Plank constant, e is electron charge, σ is conductivity (reciprocal of resistivity), N is the electron concentration in the film. The calculation results are listed in Table 1. Previous studies showed that the electron mean free path of heavily doped n-type semiconductor films is usually of the magnitude of 4 nm[14]. In this experiment, the mean free path of electrons in other samples is between 3~7 nm excepting in sample R_1, which is much smaller than film grain size. Therefore, the grain boundary scattering mechanism contributes less to the carrier mobility. The mean free path of electrons in sample R_1 is in the same order of magnitude as the grain size, so the grain boundary scattering mechanism has a considerable influence on the carrier mobility of sample R_1. On the other hand, XRD and TEM test results show that neutral SnO_2

precipitates at the grain boundaries of the film during the low deposition rate and the oxygen-rich deposition environment makes some neutral oxygen atoms adsorb at the grain boundaries of the film, which cause a certain concentration of neutral impurity scattering centers in the film. According to Erginsoy model[15], the effect of neutral impurity scattering on mobility is proportional to the concentration of neutral impurities, can be expressed by：

$$\mu_N = \frac{m^* e^3}{20\hbar^3 \varepsilon_0 \varepsilon_f N_n} \quad (5)$$

Which, $\hbar$ is the Reduce the Planck constant, ε_0 is the permittivity of vacuum, ε_f is the thin film dielectric constant, N_n is the neutral impurity concentration. Therefore, compared with sample R_2, the neutral impurity scattering mechanism in sample R_1 is relatively significant, and its carrier mobility is relatively lower.

3.3 Optical Performance

Figure 5 (a) and (b) are the transmittance curves of ITO thin films prepared at different deposition rates and oxygen flow rate in the visible spectrum (400~800 nm) (including the influence of sapphire substrate and its average transmittance in the visible spectrum is 87%). As can be seen from the figure, the main variation of visible spectrum transmittance of ITO film is to decrease with the increasing of deposition rate, and to increase with the increasing of oxygen flow rate.
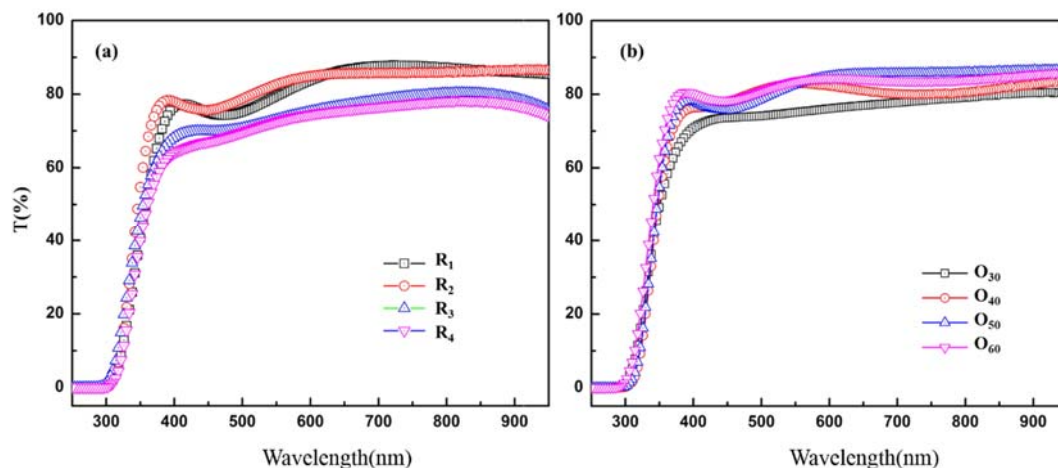

Fig.5 Transmission of as-deposited ITO thin films within visible spectrum

The energy attenuation of the ITO thin film to the light can be attributed to the scattering of photons by absorption and scattering centers. In this paper, high deposition rate and low oxygen flow rate made the films growing in a relatively oxygen-deficient environment, and nonstoichiometric In and Sn low-valent oxides formed in the film which have strong absorption of visible light result in the decreasing of visible spectrum transmittance. At the same time, the ITO thin films

prepared under the conditions of high deposition rate and low oxygen flow rate had more lattice defects and structural defects in the film have a large scattering effect on photons which reduces the transmittance of visible light.

4 Conclusion

ITO thin films were deposited on sapphire substrates under different deposition parameters via ion-assistant electron beam evaporation method. XRD test results show that the ITO thin films obtained in the experiment are all polycrystalline, the intensity of (400) plane peak, which correlated to the oxygen vacancy concentration in the film, changed with the variation of deposition conditions; Electrical performance test results show that the resistivity of the film is on the order of 10^{-4} $\Omega \cdot cm$ and the carriers were mainly derived from the oxygen vacancies formed during the film deposition and the substitutional doping of Sn^{4+} ions to In^{3+} ions in the crystal lattice. The oxygen vacancy concentration increases with the increasing of deposition rate, and decreases with the increasing of oxygen flow rate within a certain range. When the oxygen flow rate reached 60sccm during the deposition process, the increase in deposition pressure weakens the assistant energy of the O-ion beam which resulting in insufficient oxidation of the film atoms and a slight increase in the oxygen vacancy concentration. In addition, the TEM-SAED shows that neutral SnO^2 impurities are formed in the thin film at low deposition rates, which weakens the substitutional doping of Sn^{4+} to In^{3+} in the lattice and reduces the donor concentration. The carrier mobility of ITO thin film is determined by multiple scattering mechanisms. The mobility of the high carrier concentration thin film is mainly affected by the ionized impurity scattering mechanism, and the mobility decreases with the increase of the carrier concentration. However, the concentration of neutral particles in the low deposition rate film is relatively high, and the scattering effect of neutral impurities is intensified. At the same time, compared with large-scale grain film, the grain size is in the same order of magnitude as the mean free path of electron motion and grain boundary scattering has a certain influence on carrier mobility; The decrease in the visible light transmittance of the thin films is mainly due to scattering of visible light photons of absorption of light waves by low-valent In and Sn oxides formed in an oxygen-deficient deposition environment and the structural defects formed during film deposition.

References

1. WANG Xiu-juan, SI Jia-le, YANG De-lin, et al. Preparation of ITO Thin Films by RF Magnetron Sputtering at Low Temperature[J]. Journal of Synthetic Crystals, 2015, 44(06): 1516-1522.

2. JIANG Min-hong, LIU Xin-yu. Research on annealing process and properties of Al-doped ZnO films[J]. Transactions of Materials and Heat Treatment, 2009, 30(2): 53-56.

3. HUANG Jun-yi, FAN Guang-han, ZHANG Yong. Institute of Opto-electronic Materials and Technology[J], Transactions of Materials and Heat Treatment, 2010, 31(7): 25-29.

4. V. Senthilkumar, P. Vickrama*, M.Jayachandran, et al. Structure and optical properties of indium Tin Oxide (ITO) thin films with different compositions prepared by electron beam evaporation [J]. Vacuum, 2010, 84: 864-869.

5. Kwang-Hyuk Choi, Jihoon Kim, Young-Jin Noh, et al. Ag nanowire-embedded ITO films as a near-infrared transparent and flexible anode for flexible organic solar cells [J].Solar Energy Materials & Solar Cells, 2013,110:147-153.

6. Mariya Aleksandrova*, Nikolay Kurtev, Valentin Videkov, et al. Material alternative to ITO for transparent conductive electrode in flexible display and photovoltaic devices [J].Microelectronic Engineering, 2015,145: 112-116.

7. I. Del Villar*, C.R. Zamarreňo, M. Hernaez, et al. Generation of surface plasmon resonance and lossy mode resonance by thermal treatment of ITO thin-films [J]. Optics & Laser Technology, 2015,69: 1-7.

8. R.L. Weiher. Electrical properties of single crystal of indium oxide [J].Journal of Applied Physics, 1962, 33: 2834-2840.

9. Akio Suzuki, Tatsuhiko Matsushita, Takanori Aoki, et al. pulsed laser deposition of transparent conducting indium tin oxide films in magnetic field perpendicular to plume [J]. Japanese Journal of Applied Physics,2001,40: L401-L403.

10. Hiromichi ohta, masahiro orita, masahiro hirano. highly electrically conductive indium-tin-oxide thin films epitaxially grown on yttria-stabilized zirconia (100) by pulsed-laser deposition [J]. Applied Physics Letter, 2000,76(19): 2740-2742.

11. D. Mergel, W. Stass, G. Ehl, et al. Oxygen incorporation in thin films of In2O3: Sn prepared by radio frequency sputtering [J].Journal of Applied Physics,2000,88: 2437-2442.

12. V.A. Johnson, K. Lark-Horovitz. Theory of thermoelectric power in semiconductors with applications to germanium[J].Physical Review, 1953,92: 226-232.

13. S.K. Choi, J.I. Lee. Effect of film density on electrical properties of indium thin oxide films deposited by Dc magnetron reactive sputtering [J].Journal of Vacuum Science & Technology A,2001,19(5): 2043-2047.

14. Timothy J.Coutts, Thomas O.Mason, John D.Perkins, et al. Transparent conducting oxides: status and opportunities in basic research[C]. 195th Meeting of the Electrochemical Society Seattle，U.S.A Washington,1999: 6.

15. Erginsoy C. Neutral impurity scattering in semiconductor [J].Physics Review Letters,1950,79: 1013-1014.